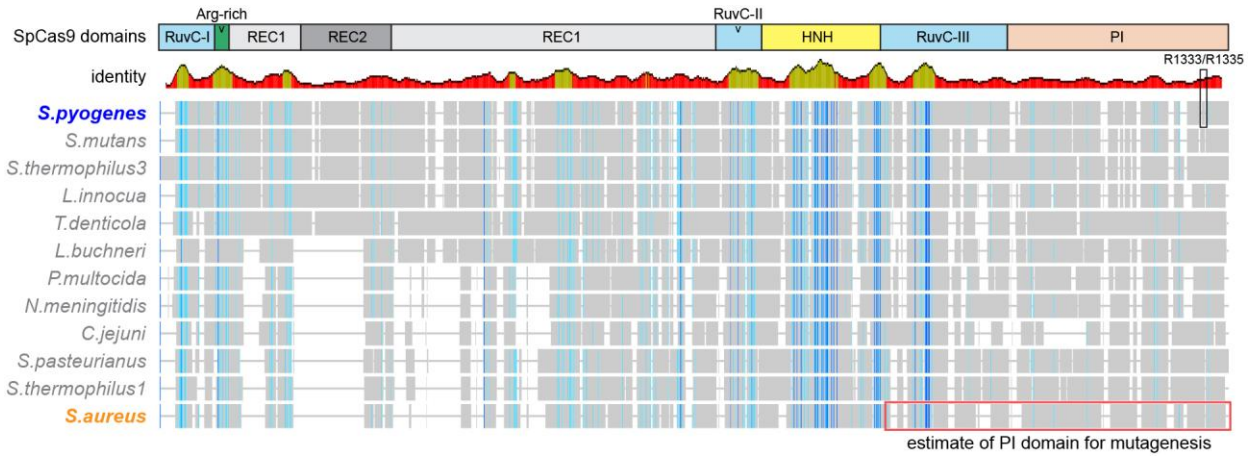


**Supplementary Figure 1**

## Protein domain alignment of Cas9 orthologues

Cas9 orthologues from **Fig. 1a** were aligned using ClustalW2. The domain structure of SpCas9 is shown at the top (based on PDB:4UN3; Anders *et al*., 2014); the PAM contacting residues of SpCas9 are highlighted; the region of SaCas9 mutagenized to select for altered PAM specificity variants is shown.


**Supplementary Figure 2**

### Primary sequence alignment of Cas9 orthologues for identification of PAM-interacting residues

SpCas9 residues previously identified (Anders *et al*., 2014; Kleinstiver *et al*., 2015) to be important for contacting the PAM are highlighted in blue, residues capable of modulating SaCas9 PAM specificity (identified in this study) are highlighted in orange, and positively charged residues adjacent to R1015 are highlighted in yellow. The structurally predicted PAM-interacting domain of SpCas9 is highlighted with a blue dashed line (based on PDB:4UN3; Anders *et al*., 2014), and the conservative estimate of the SaCas9 PAM-interacting domain used as a boundary for PCR mutagenesis is indicated with an orange dashed line.

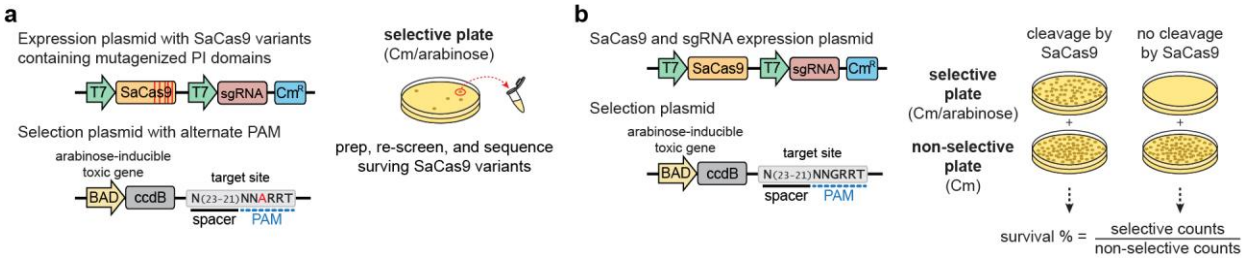


**Supplementary Figure 3**

## Schematic of the bacterial positive selection assay

(**a**) The selection plasmids can be modified to screen for Cas9 variants that are able to recognize alternative PAM sequences. (**b**) Schematic of the positive selection plasmids (left panel) and expected outcomes (right panel) when screening functional or non-functional Cas9/sgRNA pairs in the positive selection.

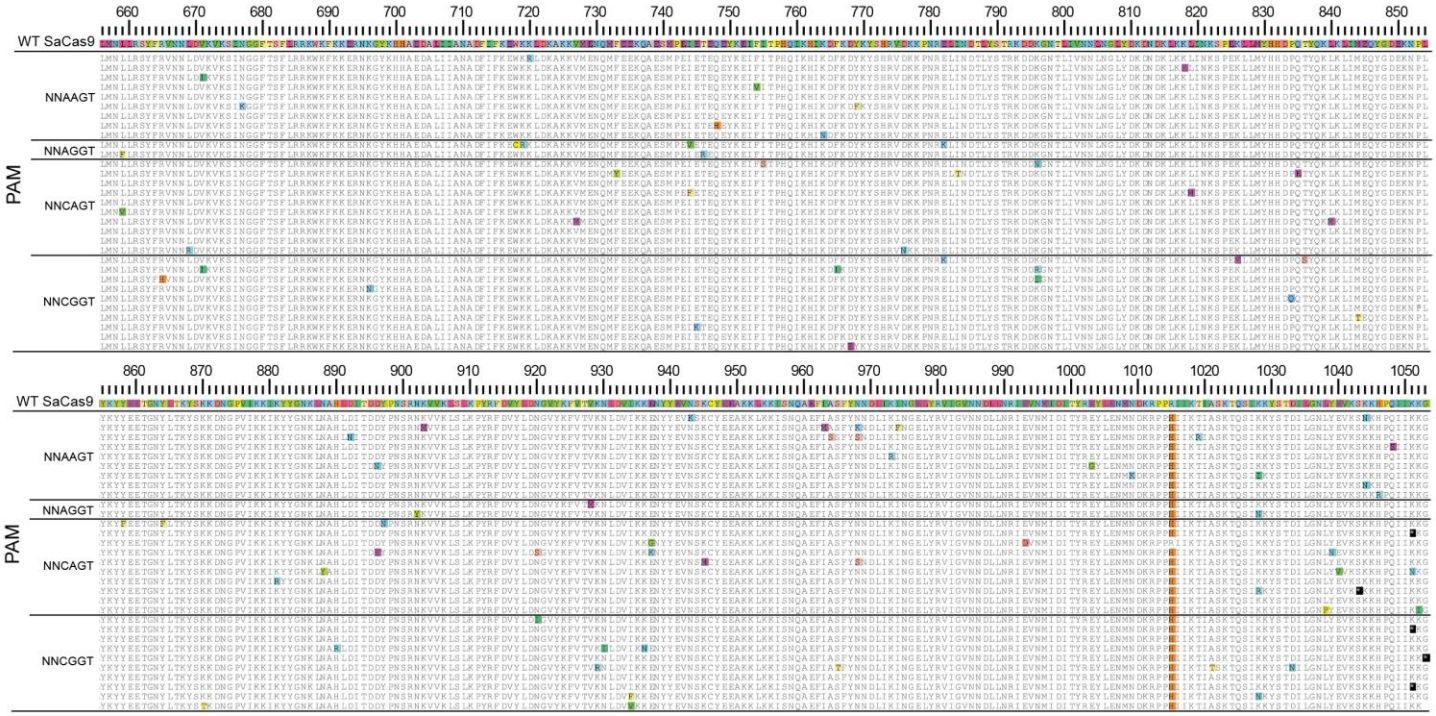


**Supplementary Figure 4**

**Amino acid sequences of SaCas9 variants that conveyed activity against non-canonical PAMs**

Selections were performed using a library derived from wild-type SaCas9 as a starting template for PCR mutagenesis. Mismatches to wild-type SaCas9 are highlighted; mutagenesis was conducted based on a conservative estimate of the PI domain (see also **Supplementary Figs. 1** and **2**).


**Supplementary Figure 5**

**Amino acid sequences of R1015Q SaCas9 variants that conveyed activity against non-canonical PAMs**

Selections were performed using a library derived from R1015Q SaCas9 as a starting template for PCR mutagenesis. Mismatches to wild-type SaCas9 are highlighted; mutagenesis was conducted based on a conservative estimate of the PI domain (see also **Supplementary Figs. 1** and **2**).

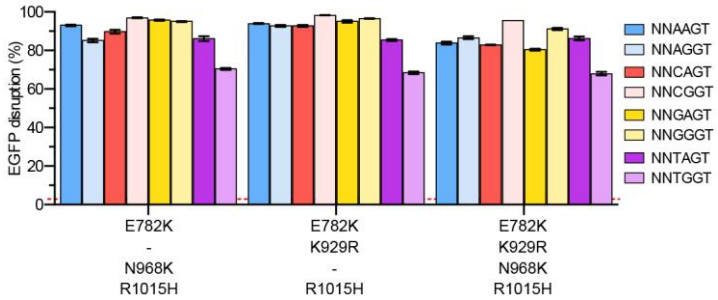


**Supplementary Figure 6**

Activity of additional SaCas9 variants

EGFP disruption activity quantified by flow cytometry; error bars represent s.e.m, n = 3, mean level of background EGFP loss represented by the dashed red line.

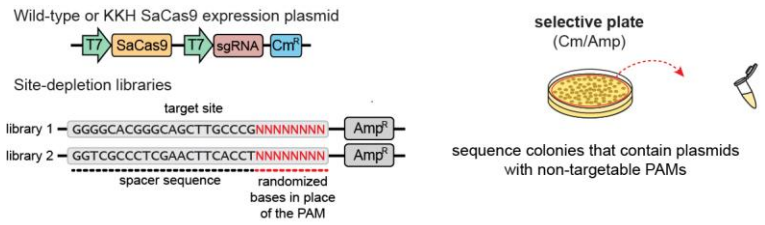


**Supplementary Figure 7**

## Schematic of the bacterial site-depletion assay

Site-depletion plasmids with 8 randomized nucleotides in place of the PAM that are refractory to cleavage by wild-type or KKH SaCas9 are sequenced. Targetable PAMs are inferred by their depletion relative to the input library, calculated as the post-selection PAM depletion value (PPDV).

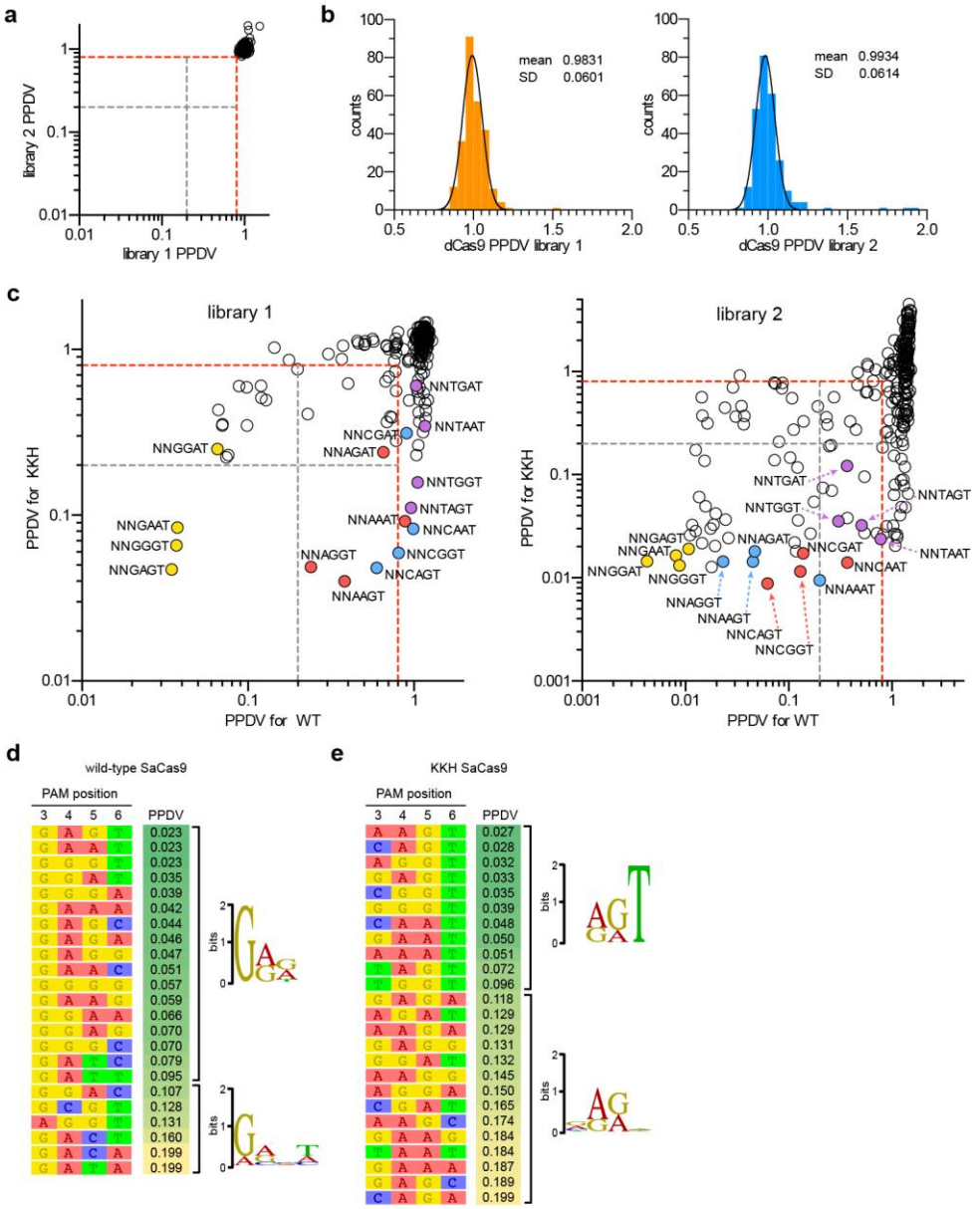


**Supplementary Figure 8**

**Site-depletion assay results for wild-type and KKH SaCas9**

(**a**) PPDV values for dCas9 control experiments on both libraries. The red dashed line indicates statistical significance (PPDV = 0.794, see **panel b**); grey dashed line indicates 5-fold depletion; PPDVs for a window comprising the 3rd/4th/5th/6th positions of the PAM are plotted (for this and **panel c**). (**b**) Statistically significant post-selection PAM depletion values (PPDVs) were determined from the dCas9 control experiments in **panel a**. Statistical significance was determined by setting the threshold at 3.36 times the standard deviation. (**c**) Comparison of the PPDVs for wild-type and KKH SaCas9 for each of the two libraries containing 8 randomized nucleotides in place of the PAM. (**d**) and (**e**) PAMs and corresponding PPDV values for all PAMs depleted greater than 5-fold for wild-type and KKH SaCas9, respectively. Sequence motifs are shown for PAMs in two categories: 1) greater than 10 fold or 2) 5- to 10-fold depleted.

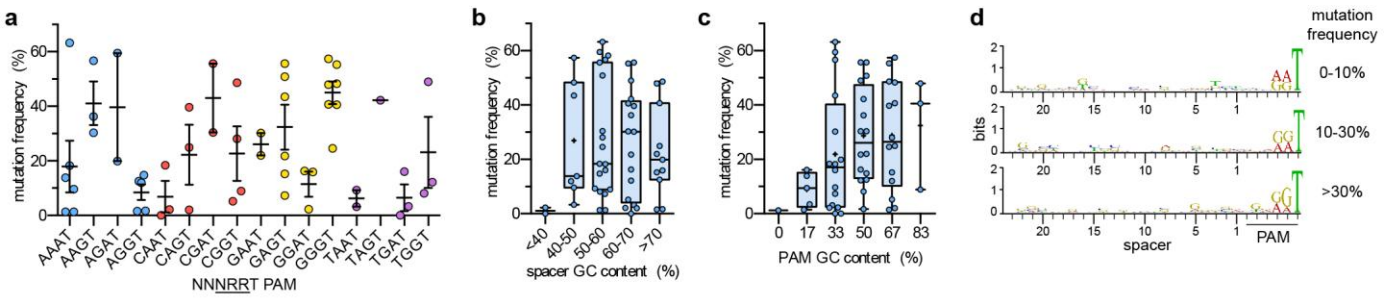


**Supplementary Figure 9**

**Additional characteristics of endogenous sites targeted by KKH SaCas9**

(**a**) Activity for each of the 55 endogenous site sgRNAs, binned based on the 16 possible NRR motifs of an NNNRRT PAM. Mean activities from **Fig. 2a** are shown for this and **panels b** and **c**. (**b**) and (**c**) Relationship between endogenous gene disruption activity and GC content of the spacer and PAM, respectively. (**d**) Sequence logos for the spacer and PAM of target sites binned based on activity. Sites were grouped based on mean mutation frequency (from **Fig. 2a**) into low (0-10%, 17 sites), medium (10-30%, 17 sites), or high (>30%, 21 sites) activity.

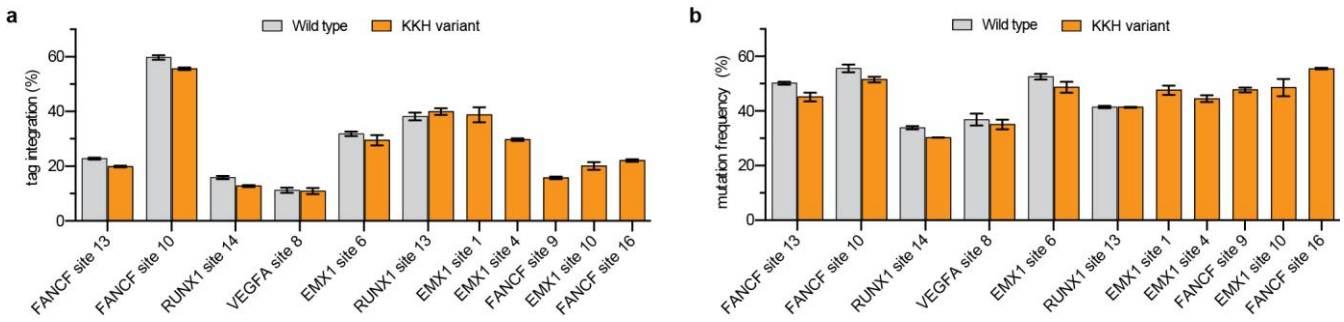


**Supplementary Figure 10**

**On-target tag integration and mutagenesis frequencies for GUIDE-seq experiments**

(**a**) Restriction fragment length polymorphism (RFLP) analysis to determine the mean GUIDE-seq tag integration frequencies. Error bars represent s.e.m., n = 3 (for this and **panel b**). (**b**) Mean mutagenesis detected by T7E1 assay.

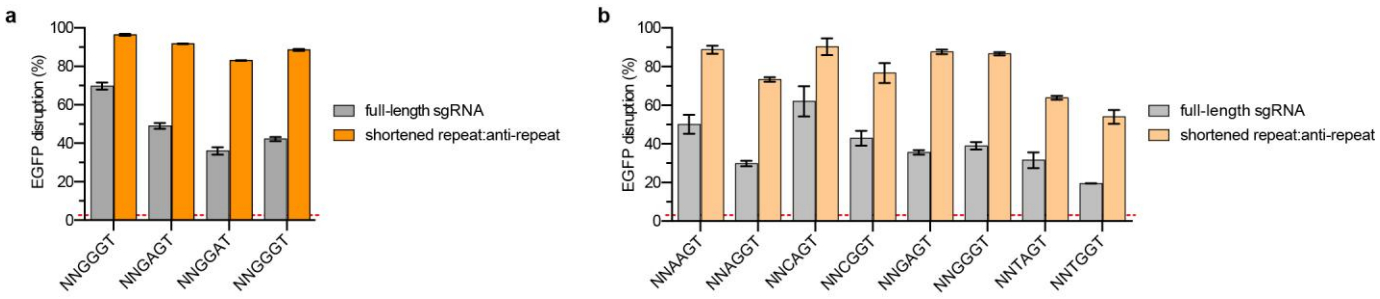


**Supplementary Figure 11**

**A truncated repeat:anti-repeat SaCas9 sgRNA outperforms the full length sgRNA**

Similar to previous results (Ran *et al.*, 2015) (**a**) Human cell EGFP disruption activity for wild-type SaCas9 against 4 sites that contain NNGRRT PAMs. EGFP disruption activity quantified by flow cytometry; error bars represent s.e.m, n = 3, mean level of background EGFP loss represented by dashed red line (for this and panel **b**). (**b**) Human cell EGFP disruption activity for KKH SaCas9 against 8 sites that contain NNNRRT PAMs.